DRAFT
CMS Physics Analysis Summary

2009/09/02
Archive Id: 0.1
Archive Date: 2009/08/24 20:47:31

Evidence for a Massive Narrow Resonance in the di-Lepton Mass Spectra in CMS

The CMS Collaboration

Abstract

Evidence for a narrow resonance has been found by the CMS Collaboration in the e^+e^- and $\mu^+\mu^-$ channels. The data correspond to 50 pb^{-1} of pp collisions at 10 TeV provided by the CERN LHC. The significance of the peak in the e^+e^- channel is 5.2σ, and in the $\mu^+\mu^-$ channel, 4.8σ. When combined, and taking systematic uncertainties into account, the significance is 7.2σ. The measured mass of the resonance is $M_{\ell\ell} = 1.24 \pm 0.15 \pm 0.04$ TeV, and the effective cross section is $\sigma \times B(pp \to X \to \ell^+\ell^-) = 21 \pm 3 \pm 2$ pb.

1 Introduction

Many models of new physics predict the existence of a narrow resonance at the TeV mass scale, decaying with substantial branching ratios to charged lepton pairs. Theoretical details can be found in numerous reviews [1].

CMS is a multi-purpose collider detector located at point 5 of the LHC at CERN [2]. Tracking is provided by silicon strip detectors and an inner pixel detector. A crystal calorimeter (ECAL) measures accurately the energy of electron and photon showers. A hadron calorimeter (HCAL) measures the energies of hadrons outside the ECAL. Both the ECAL and the HCAL are highly segmented and cover both the barrel and endcap regions. A superconducting solenoidal coil placed outside the calorimetry provides a highly uniform field of 3.8 T. Drift tubes track muons in the barrel region outside the coil, and cathode strip chambers track them in the endcaps. Resistive Plate Chambers add redundancy to the muon tracking, and a fast trigger signal. All detector systems were in good working order, similar to the performance established with cosmic rays [3].

The data used for this letter were recorded in 2010 when the LHC was delivering pp collisions at a center-of-mass energy of 10 TeV. The trigger system provides highly efficient triggers for electrons and muons with $E_T > 20$ GeV and $p_T > 20$ GeV, respectively [4]. A sample of 37 million electron triggers and 22 million muon triggers was analyzed, corresponding to an integrated luminosity of about 50 pb^{-1}. Measurements of Standard Model (SM) processes with leptonic final states have previously been published by CMS [5].

Simulated event samples were generated with standard Monte Carlo (MC) programs, including PYTHIA and ALPGEN [6]. The response of the detector was simulated in detail using GEANT [7] and parameterizations of showers and other detector response.

2 Methods

The reconstruction and calibration of electrons and muons follows standard methods [8]. The selection of events is simple, as described in the following sections.

2.1 Electrons

Electrons are reconstructed by associating a cluster in the ECAL with a track. ECAL clusters are formed by associating energy deposits in crystals surrounding a "seed", locally the highest energy, crystal into collections of crystals [10]. Track reconstruction, which is specific to electrons to allow for bremsstrahlung emission, is seeded from the clusters in the ECAL, firstly by using the cluster energy to search for compatible hits in the pixel detector and then using these hits as seeds to reconstruct a track in the Si tracker. A minimum of 5 hits are required on each track.

Electron candidates must fall within the barrel or endcap fiducial acceptance regions in pseudorapidity of $|\eta| < 1.442$ or $1.560 < |\eta| < 2.5$. The candidate electron is required to deposit most of its energy in the ECAL and relatively little in the HCAL. The energy deposits are also required to have little surrounding calorimeter activity (be isolated) within a cone of $\Delta R < 0.3$ to provide rejection of jets. A track isolation criterion is also required.

The ECAL was calibrated by using both test beam and pp collision data. Within collision data this was done by requiring symmetry in energy deposits in $r - \phi$ planes, using electrons from W bosons and finally by using electrons from the Z peak to set the overall scale. [[9]]. The

energy resolution obtained with this dataset is 1.5%.

Events are selected where at least two electron candidates have an $E_t > 25$ GeV. No further requirements are made to select events of interest, in particular, there is no requirement that the electron charges be opposite.

2.2 Muons

The highly redundant muon system allows the reconstruction of muon tracks independent of the Si tracker. Such "stand-alone" tracks are used to select good Si tracks which can be fitted together with hits in the muon chambers. In order to ensure a good quality measurement, the Si track must have at least 10 hits, and $\chi^2/N_{\mathrm{DF}} < 10$. A judicious selection of a subset of the muon chamber hits ensures the best possible muon resolution [11].

A pure sample of muons is obtained by demanding consistency of the extrapolated Si track position and the position measured in the muon chambers. Also, the energy registered by the ECAL and HCAL must be consistent with the expectation for a muon of the given energy [12]. Non-prompt muons, refered to as "fake" muons here, coming from meson decays are suppressed by imposing an isolation requirement based on the sum of the p_T of tracks within a narrow cone centered on the muon.

The momentum scale is set using the $Z \rightarrow \mu^+\mu^-$ peak and the known Z boson mass. Given 50 pb^{-1}, the relative scale uncertainty is 1.1%. When transfering this calibration to the TeV mass scale, an additional uncertainty of 3% is assigned, accounting for possible non-linear effects. The resolution at high masses is determined by the accuracy of the alignment. At a mass of 1.2 TeV, the resolution is estimated to be 7%, based on studies of residuals.

Events are selected which have two isolated muons of opposite charge and $p_T > 20$ GeV.

2.3 Efficiency Estimation

The efficiency for reconstructing and identifying good lepton candidates is measured using the "tag and probe" approach [13]. A tag lepton is established by applying tight cuts to one lepton; the other candidate is then the probe. Several factors in the overall efficiency are measured, including the trigger efficiency, Si track reconstruction efficiency, and the lepton reconstruction and identification efficiency. For electron and muon pairs, a large sample of high-purity probes is obtained from pairs with an invariant mass compatible with the Z-boson mass. The electron analysis also makes use of pairs from the Drell-Yan tail.

Using data from the Z-peak, if the probe object is required only to be a cluster in the ECAL, the efficiency of all subsequent selection criteria is found. Using only a track as the probe object allows the cluster finding efficiency to be estimated. From MC simulations the efficiency of electron identification is found to increase as a function of true energy. This becomes flat beyond about 45 GeV GeV The total efficiency measured in the data at the Z-pole is 90% $\pm$ 1.7%(barrel) and 86.8% 3.8% (endcap). The ratio of the efficiency measured from the data and the efficiency determined from MC simulation at the Z pole is found to be [YY]$\pm$ 0.017 (barrel) and [YYY]$\pm$ 0.038 (endcap). This scale factor is applied to the efficiency found for electrons with high energies determined from MC simulation to determine the efficiency used for the data sample. The systematic error is obtained by varying the estimated background under the Z peak by 50%. The total trigger efficiency is found to be 100% for events where two electron candidates pass the offline selection criteria.

The efficiency was cross checked using the events with an invariant mass greater than 120 GeV.

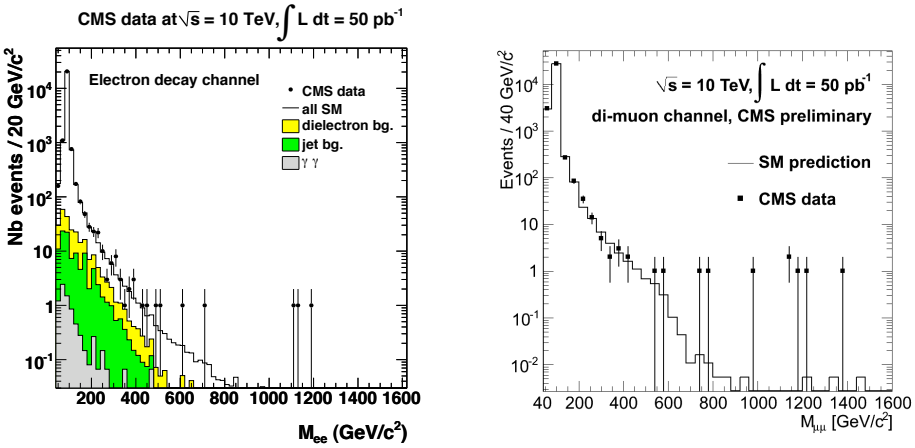

Figure 1: Invariant mass spectra for electrons *(top)* and muons *(bottom)*. The points with error bars represent the CMS data, and the histograms, the predictions based on SM processes.

The two methods agree to within statistical errors and efficiencies of $90.5 \pm 1.7\%$ (barrel) and $88.0 \pm 3.8\%$ are used throughout this paper.

A similar procedure is followed for muon, and using Z-peak data, the overall efficiency is $97.6 \pm 0.6\%$. There is no sign of a reduction in the efficiency for muon p_T up to about 150 GeV/c, beyond which there are no more events in the data. MC studies indicate that the efficiency remains constant as a function of p_T to within $\sim 1\%$, which we take as the uncertainty on the efficiency ratio of high-p_T to moderate-p_T muons.

3 Results

The compatibility of the data with SM expectations at low di-lepton masses is demonstrated first, followed by a discussion of the events at high mass.

3.1 Yields from SM processes

The most prominent contribution to the e^+e^- and $\mu^+\mu^-$ samples comes from the Drell-Yan process, with additional significant contributions from the $t\bar{t}$, tW, WW, and $Z \to \tau\tau$ processes. In addition, jets may be mis-identified as leptons, and contribute to the invariant mass spectra through QCD multi-jet and vector boson+jet processes. Lastly, di-photon events, where both photons are mis-reconstructed will contribute to the e^+e^- spectrum.

3.1.1 Backgrounds with prompt leptons

Non–Drell-Yan backgrounds with prompt leptons are estimated using two complementary methods. The processes $t\bar{t}$, tW, WW, $Z \to \tau\tau$ can give rise to any combination of lepton flavours and a sample of $e\mu$ events is used to estimate the expected e^+e^- and $\mu^+\mu^-$ distributions. About 10% of the events in this sample come from events in which a jet is mis-identified ("fakes") as an electron. This comes mainly from W+jet production. This is corrected for in this estimate of prompt leptons.

The second method applies b-tagging to the di-lepton event sample to estimate the contribution from top events ($t\bar{t}$ and tW). The b-tagging efficiency is estimated by comparing the number of

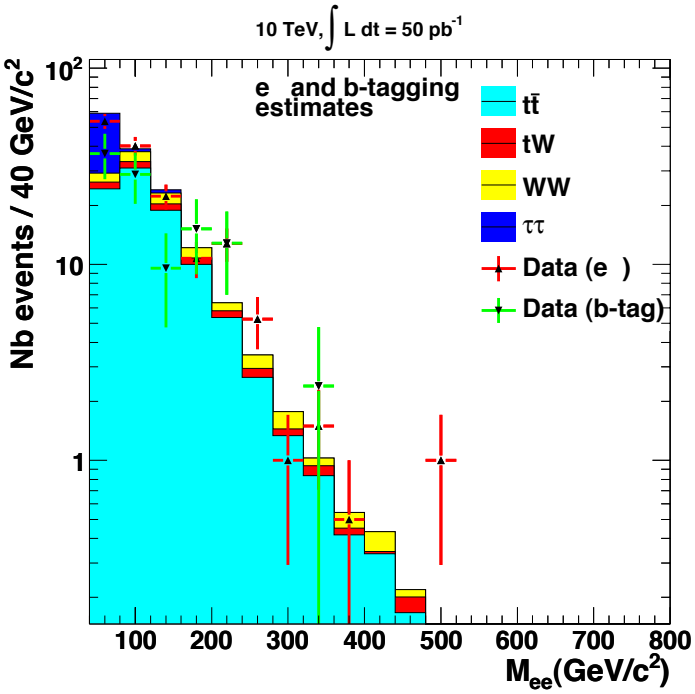

Figure 2: The solid histrogram shows the Monte Carlo simulation of the contribution to the di-electron invariant mass spectrum from $t\bar{t}$, tW, WW and $Z \to \tau\tau$ processes. The red data points result from the $e\mu$ estimation method and the blue from the b-tagging method. The b-tagging method does not estimate contributions from the WW or $Z \to \tau\tau$ processes.

single-tagged and double-tagged events, with corrections for acceptance and the contribution of tW events taken from simulations.

The $e\mu$ and the b-tagging estimates are statistically independent, and suffer from different systematics. Fig. 2 shows the agreement of the estimates, indicating that this background contribution is understood well. Note that $Z \to \tau\tau$ events only contribute to the $e\mu$ estimate. The events predominantly contribute outside of the control region between 120-600 GeV. No correction for this contribution is therefore made to the b-tag estimate of the prompt lepton background.

3.1.2 Fake leptons

The probability for a jet to be mis-identified as a lepton has been measured using data samples obtained with pre-scaled jet triggers. The lowest accessible jet threshold is 30 GeV. The so-called "fake rate" is computed in bins of E_t or p_T as the numbers of jets passing the lepton selection requirements divided by the total number of jets. For electrons used in this analysis, the fake rate is estimated to be $(0.04 \pm 0.01) \times 10^{-3}$ in the barrel and $(0.3 \pm 0.1) \times 10^{-3}$ in the endcap for a jet with E_t around 200 GeV. For muons, the corresponding number is $(xx \pm yy) \times 10^{-4}$. The errors are statistical.

The mass spectrum of backgrounds events with at least one fake lepton is obtained from an event sample with one object passing all lepton selection criteria, and no other such object. There must also be a suitable jet. The Drell-Yan contribution to this sample is negligible. The E_t (p_T) of the jets in this sample are weighted by the fake rate, and the invariant mass is calculated. This spectrum includes the background from purely multi-jet processes and from a vector boson+jet(s). A systematic uncertainty of 50% is assigned to account for errors due to converting

jet E_t into electron E_t or muon p_T, and the composition of this sample. The spectrum obtained is shown in Fig. 1.

The di-muon signal sample contains only muon pairs of opposite electric charge; background events with non-prompt muons will contain same-charge pairs which can be used to check the predicted level of such backgrounds. There are 3 events with same-charge muon pairs and $M_{\mu\mu} > 120$ GeV, compared to 2 ± 1 events predicted.

3.2 Cosmic Ray Muons

The di-muon sample is susceptible to contamination from cosmic ray muons, which can be reconstructed as a pair of oppositely-charged, high-momentum muon tracks. The contribution from cosmic ray muons was estimated using several topological and kinematic criteria, including the impact parameter, acollinearity, momentum balance, and arrival time of the muon with respect to other tracks in the event. The rate and mass spectrum was established through an analysis of cosmic ray runs (see Ref. [3]), and the number of events in the final sample was estimated based on the integrated live time of the experiment during the runs used in the di-muon analysis. For $M_{\mu\mu} > 800$ GeV, the expected number of cosmic ray muon events is less than 0.1 event.

3.3 di-Lepton Spectra

Figure 1 shows the di-lepton mass spectra obtained from CMS data. These are compared the SM expectation based on multi-jet backgrounds estimates directly from the data, and MC simulations of other processes. Good agreement is observed for masses below several hundred GeV.

Searches for narrow resonances at the Tevatron have placed limits in the mass range 600 GeV to 800 GeV [14]. A control region expected to be free of any new physics signal is defined (indicated by the arrow in Fig. 1): to be 120 GeV $< M_{\ell\ell} <$ 600 GeV. The good agreement between the data and the prediction confirms that the SM expectations and the detector performance are well understood. Kolmogorov-Smirnov tests were calculated between the observed spectrum and the prediction; the probabilities are 63% for electrons and 41% for muons.

The total number of events observed in this mass range is 421 for the electron channel and 478 for the muon channel. The number estimated to come from prompt leptons using the $e\mu$ method is 41 ± 3 (stat) ± 7 (syst) (electrons) and 52 ± 8 (muons). The contribution where at least one jet fakes a lepton is measured using the method described above for electrons and is 18 ± 9 events. This agrees well with the number of Drell-Yan events expected in this region of 329 ± 13 (electrons) and 480 ± 17 events for muons, where the error is due to the pdf uncertainty.

3.4 Cross Checks

The events above 800 GeV are rare, and it is important to check the response of the detector at these scales.

3.4.1 ECAL cluster energies

The maximum energy deposited in a crystal which is part of the clusters associated with the candidate events close to 1.2 TeV is significantly larger than the energies in the data used for calibration where data originating from Z boson decay, are used. The energy of a 5x5 cluster of crystals can be determined excluding the information from the highest energy crystal and using a knowledge of the lateral shower shape. A precision of between 4-9% is expected using this

Table 1: Salient kinematic properties of the events displayed in Fig. 3

channel	mass (TeV)	energies (GeV)
e^+e^-	1.18 ± 0.22	780 , 330
$\mu^+\mu^-$	1.24 ± 0.41	1244 , 812

Table 2: Excesses observed for $M_{\ell\ell} > 800$ GeV. N_{pred} is the predicted number of events from SM processes, including total uncertainty. N_{obs} is the observed number of events.

channel	N_{pred}	N_{obs}	p-value
e^+e^-	0.22 ± 0.10	4	3.8×10^{-6}
$\mu^+\mu^-$	0.36 ± 0.18	5	2.4×10^{-6}
combined	0.58 ± 0.21	9	3.3×10^{-9}

procedure. Using events with an invariant mass below 600 GeV confirms that this precision is achieved.

The cluster energies for the events in the signal region are determined using this procedure and the energies obtained are [we would quote the specific energies here].

3.4.2 Muon chamber signals

The properties of the tracks detected in the muon chambers were examined to make sure they correspond to the expectation for high-energy muons. Similarly, the energies in the ECAL and HCAL were checked, to exclude the possibility of a high-energy hadron punching through the calorimetry.

Further checks against cosmic ray muons were performed, based on the distribution of the impact parameter, the acollinearity, and timing of the muon signals with respect to other tracks in the event. These checks confirm a negligible contribution from cosmic ray muons.

3.4.3 Scrutiny of events

The individual events with $M_{\ell\ell} > 800$ GeV were scrutinized to check for signs of detector malfunction or reconstruction errors. **bulk this up**

There is no evidence of any defect in the events at high mass.

Displays of events from both channels are shown in Fig. 3. Some salient kinematic properties of these two events are listed in Table 1.

3.5 Significance

An excess of events is observed in both the e^+e^- and $\mu^+\mu^-$ channels, clustered around 1.2 TeV. Predictions can be made of the numbers of events with $M_{\ell\ell} > 800$ GeV, based on MC simulations of SM processes. Table 2 summarizes these predictions, the observations, and the p-values [1]. The combined p-value is 3.3×10^{-9}, corresponding to a 7.2σ significance.

Two scans for narrow resonances were performed over the mass range $[800, 2000]$ GeV in the e^+e^- and $\mu^+\mu^-$ channels separately. The signal shape is given by the detector resolution (Sec. 2.1,2.2) and a radiative tail, assuming a negligible total width for the resonance. The

[1] Given a mean expected number of events, the p-values is the probability that the number of events observed in any one experiment matches or exceeds the number that is observed.

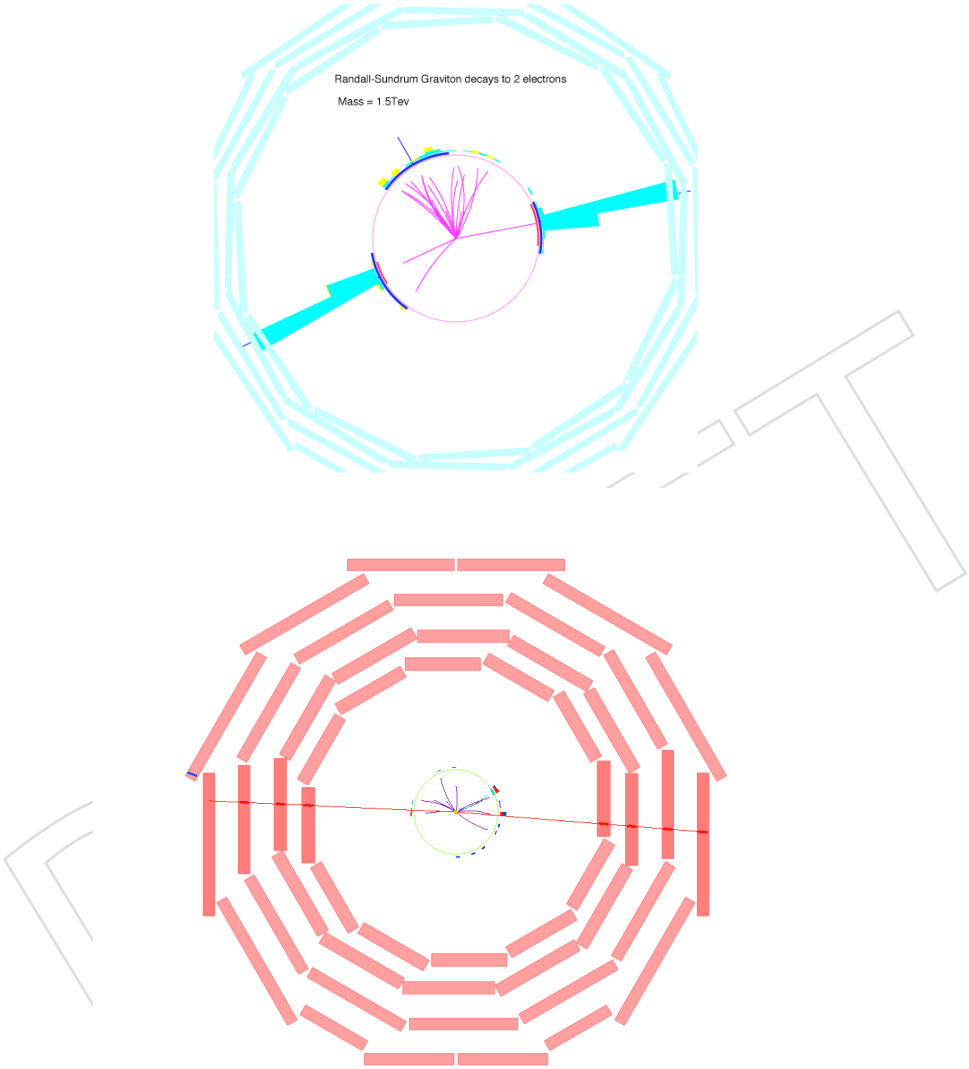

Figure 3: Displays of an e^+e^- event *(top)* and a $\mu^+\mu^-$ event *(bottom)*

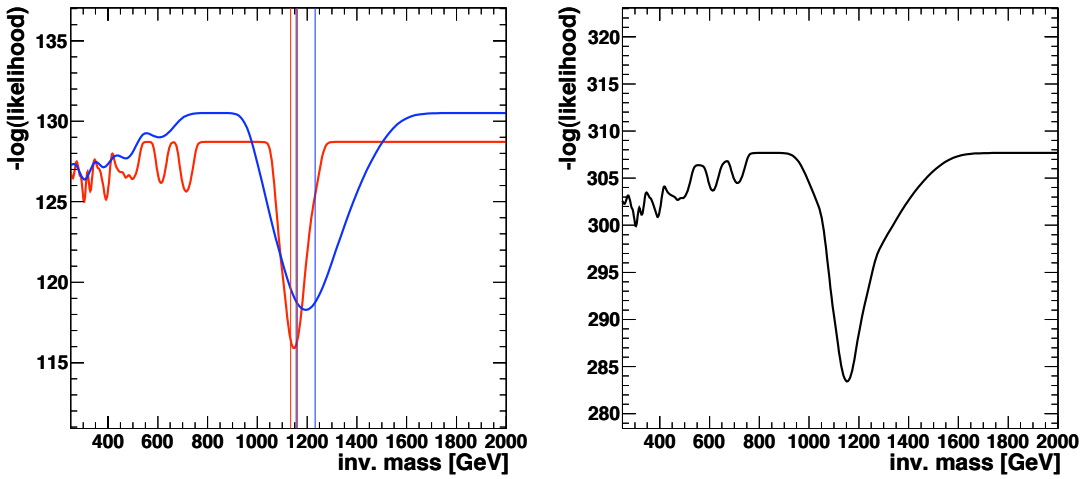

Figure 4: Scans for narrow resonances in the electron and muon channels *(top)*, and for both channels combined *(bottom)*.

negative logarithm of the ratio of likelihoods, $\xi = -\ln[\mathcal{L}_{s+b}/\mathcal{L}_b]$, was used as the test statistic, where b refers to the background hypothesis and $s+b$ refers to the background plus signal hypothesis; the signal is parametrized by a mass and an amplitude. The amplitude ($S_{\rm NP}$) was parametrized by a number of events ($N_{\rm NP}$) relative to the number of selected events at the Z-pole (N_Z):

$$S_{\rm NP} = \left(\frac{N}{A\varepsilon}\right)_{\rm NP} \cdot \left(\frac{A\varepsilon}{N}\right)_Z . \tag{1}$$

Here, the subscript NP refers to the signal, while Z refers to leptons from the Z peak defined by 60 GeV $< M_{\ell\ell} <$ 120 GeV; the ratio of efficiencies was discussed in Section 2.3 and the ratio of acceptances is calculated with MC simulations, with the assumption that the new physics comes from a resonance of spin-1. This amplitude requires no knowledge of the integrated luminosity. The scans are shown in Fig. 4. Evidence for a significant excess is observed near 1.2 TeV in both channels. The probability for observing a statistical fluctuation anywhere in the scanned mass range was taken into account using toy MC tests; the consequent significanes are 3.7σ for the electron channel, and 3.6σ for the muon channel.

The largest amplitudes occurs near 1.2 TeV in both channels: $S^{ee}_{\rm NP} = (1.8 \pm 0.3) \times 10^{-3}$ in the e^+e^- channel, and $S^{\mu\mu}_{\rm NP} = (1.6 \pm 0.4) \times 10^{-3}$ in the $\mu^+\mu^-$ channel. The difference in normalized yields, $\Delta S = S^{ee}_{\rm NP} - S^{\mu\mu}_{\rm NP} = (0.2 \pm 0.5) \times 10^{-3}$, is consistent with zero. The probability to observe this value of $|\Delta S|$ or larger is 78%, if the two peaks comes from the same particle, according the MC simulations.

The shape of the test statistic ξ can be used to infer a best value for and uncertainty on the mass. The scans give $M_{ee} = 1.24 \pm 0.02 \pm 0.08$ TeV and $M_{\mu\mu} = 1.19 \pm 0.07 \pm 0.02$ TeV, where the first uncertainty is statistical and the second is an estimate of the scale uncertainty. The difference in these values is $\Delta M = M_{ee} - M_{\mu\mu} = 0.05 \pm 0.07 \pm 0.08$ TeV. MC simulations show that the probability to observe this value of $|\Delta M|$ or larger is 77%, if the two peaks come from the same particle.

The two measured mass values can be combined using the BLUE method [16], assuming that the mass peaks come from the same particle. Taking systematic uncertainties into account, the

result is

$$M_{\ell\ell} = 1.22 \pm 0.04 \pm 0.08 \text{ TeV}, \quad (2)$$

where the first uncertainty is statistical and the second represents the uncertainties on the mass scales.

A combined scan was performed. The test statistic was based on the product of the likelihoods, and Gaussian constraints on the mass scale uncertainties. The amplitudes were constrained to give the same effective branching ratio for each channel. At each mass the values maximinzing the test statistic were found and the bottom plot in Fig. 4 shows the result of the combined scan. The significance for the combination of electon and muon channels is 5.9σ.

The combined scan yields the amplitude $S_{\text{NP}}^{\ell\ell} = (1.73 \pm 0.14) \times 10^{-3}$. A value for the effective cross section for new physics can be deduced from this value according to $\sigma_{\text{NP}} = \sigma_{\text{Z}} \times S_{\text{NP}}$. Taking $\sigma_{\text{Z}} = 1.87 \pm 0.03$ nb [17] gives

$$\sigma \times B(pp \to X \to \ell^+\ell^-) = 21 \pm 3 \pm 2 \pm 1 \text{ pb} \quad (3)$$

where the first uncertainty is statistical, the second includes experimental uncertainties such as the efficiency, and the third reflects the theoretical uncertainties on σ_{Z}.

It is not possible to make a significant conclusion about the spin of the new resonance on the basis of the current data sample.

4 Conclusion

Evidence for a new narrow resonance has been found in the CMS data corresponding to an integrated luminosity of 50 pb^{-1} taken at a center-of-mass energy of 10 TeV. Narrow peaks are observed near 1.2 TeV in both the e^+e^- and $\mu^+\mu^-$ channels. A combined scan of these channels was used to obtain a mass measurement $M_{\ell\ell} = 1.22 \pm 0.03 \pm 0.08$ TeV. The yields support the hypothesis of equal branching ratios. With the assumption that one particle is responsible for both peaks, and that the branching ratios are equal, a cross section $\sigma \times B(pp \to X \to \ell^+\ell^-) = 21 \pm 3 \pm 2$ pb has been measured.

Larger data samples will allow more precise measurements of the mass and effective cross section, and to deduce the spin of the new resonance.

Acknowledgments

We thank the whole world for their support.

References

[1] a list of good theory reviews

[2] CMS TDR, or some other detailed detector description

[3] The volume of CRAFT papers

[4] CMS uses a traditional coordinate system with the z axis running along the beam, x defining the horizontal coordinate and y defining the vertical. The origin is at the geometric center of the tracker. E_T is the transverse energy of an electron or jet, and p_T is the transverse momentum of a track, including muons. The pseudo-rapidity is $\eta = -\ln[\tan(\theta/2)]$.

246 [5] list of relevant lepton-based publications from CMS

247 [6] standard references to Pythia, Alpgen, and other event generators used in this analysis

248 [7] GEANT reference

249 [8] references to published papers explaining standard methods for reconstructing and cali-
250 brating electrons and muons.

251 [9] reference to ECAL calibration method and measurement

252 [10] reference for ECAL crystals and electron reco

253 [11] reference for the reco muon cocktail

254 [12] Very energetic muons, such as those found here, have a significant probability to interact
255 in the calorimeters. The cut on calorimeter energies is therefore scaled ...

256 [13] reference for tag-n-probe methods

257 [14] recent Tevatron publications setting limits on narrow resonances

258 [15] The expected yields are calculated based on an NNLO cross section calculation: $\sigma =$
259 $xxxx \pm yyyy$ pb. [reference for the SM NLO value for the high-mass DY.]

260 [16] reference for the BLUE method of combining measurements

261 [17] reference for the SM value for the Z peak (60,120)

262 [18] Carena et al. paper giving the (c_d, c_u) formalism.